Design and experiment analysis of the small maize harvester with attitude adjustment in the hilly and mountainous areas of China

Meizhou Chen[1], Guangfei Xu[1,2], Yuanzhen Wei[3], Yinping Zhang[1], Peisong Diao[1*], Huanxiao Pang[1]

(1. *College of Agricultural Engineering and Food Science, Shandong University of Technology, Zibo 255000, Shandong, China*;
2. *School of Mechanical and Automotive Engineering, Liaocheng University, Liaocheng 252000, Shandong, China*;
3. *Shandong Academy of Agricultural Machinery Sciences, Jinan 250000, China*)

Abstract: To solve the problem of small planting plots and large sloping land for mechanized maize harvesting in China hilly and mountainous areas, a small maize harvester with attitude adjustment was designed to realize maize snapping, peeling, straw crushing and attitude adjusting at on time in this study. The basic structure and working principle of the small maize harvester were described, and the key components were designed as follows. The maize snapping device adopted the combination form of maize snapping plates and straw pulling rollers, and the gap of the straw pulling rollers can be adjusted to adapt to different maize varieties. Two pairs of peeling rollers formed a groove arrangement to improve peeling rate and reduced ear grain loss. The pressure feeding device mainly comprised drive chain and three grade pressure feeding rollers to increase the friction between ears and the peeling rollers, and help ears slide. The attitude adjustment advice was designed according to the high point stationary pursuit leveling method. When the attitude angle of the rack approached 0, the small maize harvester reached the level state. The actual range of attitude adjustment was obtained and the accuracy of static attitude adjustment was verified through attitude adjustment test. The influencing factors of ear loss rate and bract peeling rate were determined by orthogonal test, including the rotational speed of straw pulling rollers, peeling rollers and pressure feeding rollers. The mathematical regression model between the experimental factors and indicators was established by using Design Expert, and through the analysis variance to verify the significance of the evaluation indicators, the best combination of operation parameters was determined that the rotational speed of straw pulling rollers, peeling rollers and pressure feeding rollers were 1440 r/min, 1535 r/min and 406 r/min. Under the optimal combination of the operation parameters, the ear loss rate and bract peeling rate were 1.33% and 93.98%. The design indicators of the small maize harvester can meet the relevant national standards, and can satisfy the need of maize mechanized harvesting in China hilly and mountainous areas.

Keywords: maize, harvester, hilly and mountains areas, attitude adjustment, anti rollover structure
DOI: 10.25165/j.ijabe.20241701.7596

Citation: Chen M Z, Xu G F, Wei Y Z, Zhang Y P, Diao P S, Pang H X. Design and experiment analysis of the small maize harvester with attitude adjustment in the hilly and mountainous areas of China. Int J Agric & Biol Eng, 2024; 17(1): 118–127.

1 Introduction

China's hilly area accounts for about 60% of the total cultivated area[1]. Because of the large fluctuation of land, scattered farmland, difficult roads, the development of agricultural mechanization in hilly areas is slow, which is the weak area of agricultural mechanization development in China[2,3]. At present, small and sloping plots are the main planting areas of maize in China hilly and mountainous areas[4,5]. The maize harvester for large-scale in Huang-huai-hai and northeast China has poor adaptability and matching in hilly and mountainous areas[6-8]. In addition, the existing small harvesters have the problems of low harvesting efficiency, high harvesting loss, poor climbing performance, easy rollover and other safety hazards[9,10].

In view of the problems of maize mechanization harvesting difficulty in hilly areas, domestic scholars have done researches on small maize harvesters for hilly and mountains terrain. The CSX 7050 mountain maize harvester from New Holland can ensure the horizontal plane of the harvester under complex terrain conditions[11]. The horizontal plane of the harvester can be maintained by controlling two independent hydraulic systems of horizontal correction and vertical correction and supporting corresponding sensors[12]. However, foreign large maize harvesters are difficult to adapt to the harvester needs of small plots[13]. Domestic self-propelled maize harvesters suitable for mountainous operations can only adapt to small-slope plowing operations in an inclined state[14].

Domestic scholars have carried out researches related to miniature suspended maize harvester based on walk-behind tractor. Wang et al.[15] developed a 4YW-1 miniature maize harvester matching with walking tractor, but it was easy to lose harvest due to the high distance between the horizontal picking roller and the ground. Zhang et al.[16] developed a double-row maize harvester matched with walking tractor, but the supporting power of this machine was small, so it can only realize the process of snapping ears, and the operating efficiency needs to be improved. Xu et al.[17] developed a single row maize harvester, and studied the technology of maize snapping, transportation and peeling with low dip angel and low loss without branch. However, due to the relatively

Received date: 2022-04-13 **Accepted date:** 2023-11-07
Biographies: Meizhou Chen, PhD, Lecturer, research interest: new agricultural machinery and equipment, Email: chenfeng2830@163.com; **Guangfei Xu**, PhD, research interest: intelligent agricultural manufacturing, Email: xuguangfei@lcu.edu.cn; **Yuanzhen Wei**, MS, research interest: agricultural machinery, Email: 549460141@qq.com; **Yinping Zhang**, Associate Professor, research interest: agricultural machinery, Email: zhangyinping929@163.com; **Huanxiao Pang**, MS candidate, research interest: agricultural machinery, Email: 2944724121@qq.com.
***Corresponding author: Peisong Diao**, PhD, Professor, research interest: agricultural mechanization engineering. College of Agricultural Engineering and Food Science, Shandong University of Technology, Zibo 255000, Shandong, China. Tel: +86-13864306142, Email: dps2003@163.com.

unreasonable structure, the loss of ear and grain was large. Li et al.[18] designed a small harvester driven by the chassis of a micro-cultivator, which solved the problem of maize harvesting inter-cropping mode. These maize harvesters can solve the needs of maize harvesting in hills and mountains to a certain extent. However, due to the large slope of cultivated land in some areas, these small maize harvesters are prone to tipping over, resulting in low harvesting. Therefore, developing a small harvester with attitude adjustment adapting to hilly terrain and high operating efficiency is the key to solve the above problems.

In China, the application of automatic leveling control technology in the field of agricultural machinery began relatively late, the scope of application is relatively narrow, mainly focusing on the leveling of farm graders, mountain tractors, orchard machinery and tractor suspension implements[19]. There is no relevant research and application in leveling the body of maize harvesting machinery. The position error-based leveling strategy has smaller error and shorter leveling time, which is more suitable for real-time leveling during harvesting operations. Leveling strategies based on position error can be broadly categorized into three types: leveling-by-low, leveling-by-high, and leveling without moving the center point[20].

Therefore, to solve the above problems, a small maize harvester with attitude adjustment for hilly and mountains areas was designed to realize the body leveling on the slope with the position error-based leveling strategy and ensure low-loss harvest of maize. The device provides theoretical and technical reference for the R&D of similar devices for maize harvester.

2 Main structure and working principle

2.1 Main structure

Based on the maize planting agronomic requirements and complex terrain environment in China hilly and mountainous areas, a small maize harvester with attitude adjustment was designed, comprising frame, feeding chains, maize snapping device, straw crushing device, pressure feeding device, peeling device, ear box, attitude adjustment device and other accessory parts, as shown in Figure 1.

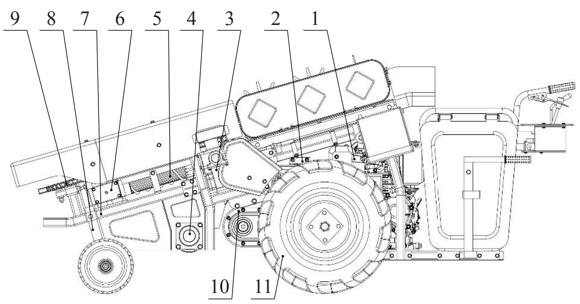

a. Front view

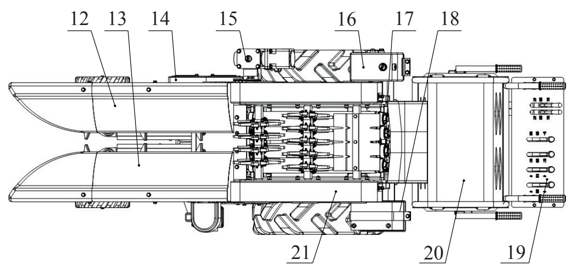

b. Top view

1. Diesel engine 2. Traveling transmission 3. Snapping and peeling transmission 4. Straw crushing device 5. Maize snapping device 6. Feeding reduction gear 7. Frame 8. Front supporting tires 9. Feeding chain 10. Attitude adjustment device 11. Back road wheel 12,13. Protective cover 14. Drive system 15. Hydraulic pump 16. Hydraulic oil tank 17. Peeling device 18. Battery 19. Control board 20. Ear box 21. Pressure feeding device

Figure 1 Structure diagram of small maize harvester with attitude adjustment in China hilly and mountain areas

During operation, attitude adjustment device calibrates maize harvester posture. The maize plants are transported backwards by feeding chain in sequence. Corn snapping device realizes separation of maize ear and straw. Pressing feeding device and peeling device realizes separation ears and bracts. Straw crushing device realizes separation of straw and stubble, and crushing of straw. Main parameters of small maize harvester are listed in Table 1.

Table 1 Main parameters of small maize harvester

Parameters	Values
Size of the machine (length×width×high)/mm³	2500×850×1060
Matched power/kW	8.0
Number of working rows	1
Working speed/m·s⁻¹	0.6
Adaptive row spacing/cm	60

2.2 Design of maize snapping device

The maize snapping device is mainly composed of a pair of horizontal straw pulling rollers, maize snapping plates and feeding chains with picking teeth, as shown in Figure 2. Compared with the snapping rollers, the snapping plates can reduce the “gnawing injury” on ear butt and achieve the purpose of reducing grain loss. During harvesting, the feeding chains guide the maize plant into the maize picking region, then the straw pulling rollers rotates opposite to each other and pull the straw downward. At the same time, the maize snapping plates forcibly snap the maize ear to complete the maize snapping process.

The clearance adjustment of straw pulling rollers can be realized by the coordination of spherical drive shaft and pin shaft to adapt to the change of straw diameter. Therefore, the versatility of the small maize harvester can be improved. The straw pulling rollers should be able to grasp the straw without grasping the ear. Therefore, the diameter of the straw pulling roller should meet:

$$\frac{d_s-\tau}{1-\frac{1}{\sqrt{1+\mu_s^2}}}\le D\le\frac{d_e-\tau}{1-\frac{1}{\sqrt{1+\mu_e^2}}} \tag{1}$$

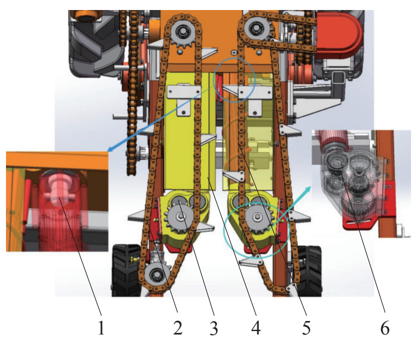

1. Spherical drive shaft 2. Feeding chains 3. Reduction gearbox 4. Maize snapping plates 5. Straw pulling rollers 6. Straw pulling rollers guideway

Figure 2 Structure diagram of feeding and snapping device where, d_s is the diameter of maize straw, mm; d_e is the diameter of maize ear, mm; τ is the clearance of straw pulling rollers, mm; D is the diameter of straw pulling rollers, mm; μ_s is the grabbing coefficient of straw by straw pulling rollers; μ_e is the grabbing coefficient of maize ear by straw pulling rollers. Generally, μ_s and μ_e are 0.7-1.1; τ is 12-17 mm; d_s is 50-58 mm; d_e is 20-25 mm; the diameter d_e measured is 25.9-27.2 mm[21]. According to Equation (1), the diameter of straw pulling rollers can be calculated as 45 mm≤ D≤319 mm. Combined with the actual situation[18], the diameter of straw pulling rollers D is designed as 52 mm.

The pulling length of the straw pulling rollers should ensure that the highest and lowest ear parts of maize should be snapped, while the straw are completely pulled down at the end of straw pulling roller. The working process of maize snapping is shown in Figure 3. The minimum pulling length of the straw pulling rollers should satisfy the following condition:

$$\begin{cases} L\cos\eta = l_1 + l_2 \\ \dfrac{l_1 + l_2}{\omega r \sin\eta + v} \geq \dfrac{h}{\omega r \cos\eta} \end{cases} \tag{2}$$

where, L is the working length of straw pulling roller, mm; l_1 is the forward distance of small maize harvester, mm; l_2 is the distance of maize plant moving backward, mm; ω is the angular velocity of straw pulling roller, rad/s; r is the radius of straw pulling roller, mm; η is the horizontal angle of straw pulling roller, (°); h is the distance between the top of plant and the location of snapping, mm; v is the forward velocity of small maize harvester, m/s. According to maize planting agronomy, the plant height is 1600-3000 mm; the ear height is 900-1300 mm, thus h is 1100-2700 mm; the distance between the front end of straw pulling roller and ground is designed as 300-480 mm; Learn from relevant research experience[22], horizontal angel η is usually 15°-30°; forward velocity v is 0.6 m/s; angular velocity ω is 170 rad/s. According to Equation (2) and combined with the actual situation, the working length of straw pulling roller is calculated to be 350 mm.

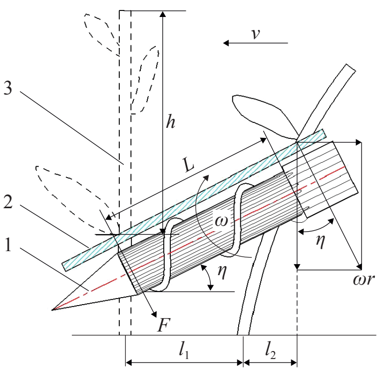

Note: F is the force of straw pulling rollers on straw, N.

1. Straw pulling rollers 2. Maize snapping plates 3. Maize plant

Figure 3 Working process diagram of maize snapping device

To achieve the ideal working effect of maize snapping device and reduce the snapping damage, it is necessary to analyze the process of snapping ear by mechanics, as shown in Figure 4.

For the effective snapping of ear without low damaging them, it should meet the following conditions:

$$\begin{cases} P_{by} = P_b \sin\lambda_1 \\ T_{by} = T_b \sin\lambda_2 \\ T_{by} - 2P_{by} > 0 \end{cases} \tag{3}$$

where, P_b is the resultant force of maize snapping plate on maize ear, N; P_{bx} is the component force of maize snapping plate on maize ear horizontally, N; P_{by} is the component force of maize snapping plate on maize ear vertically, N; T_b is the resultant force of straw pulling roller on the straw, N; T_{bx} is the component force of straw pulling roller on the straw horizontally, N; T_{by} is the component force of straw pulling roller on the straw vertically, N; λ_1 is the angle between P_b and the horizontal direction, (°); λ_2 is the angle between T_b and the horizontal direction, (°).

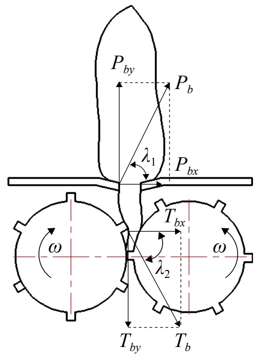

Figure 4 Force analysis on maize ear

It can be seen that the effect of snapping ear can be improved by increasing the component force of straw pulling roller on the straw vertically. Therefore, in order to increase the friction of straw on the straw pulling roller, grooves are milled on the roller, and the length of which was 260 mm.

2.3 Design of peeling device

In order to make the ear on the peeling roller more conducive to rotation around its own axis and all the bracts are stripped clean, two peeling rollers configuration should be a height difference. The force analysis of peeling roller and ear is shown in Figure 5.

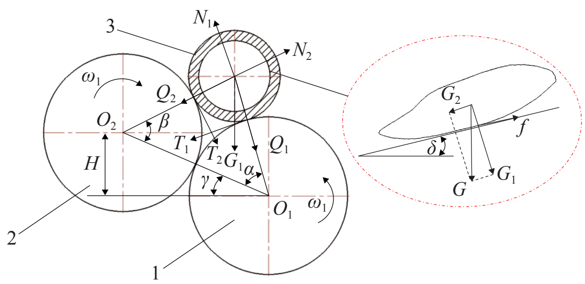

1. Down peeling roller 2. Up peeling roller 3. Ear

Figure 5 Force analysis

It can be seen from Figure 5 that the positive force of ear on peeling rollers are as following respectively

$$\begin{cases} Q_1 = \dfrac{G\cos\delta\cos(\alpha - r)}{\sin(\beta + \alpha)} \\ Q_2 = \dfrac{G\cos\delta\cos(\alpha + r)}{\sin(\beta + \alpha)} \end{cases} \tag{4}$$

where, Q_1 and Q_2 are the positive force of ear on peeling rollers, respectively, N; G is the gravity force of ear, N; δ is the inclination angle of peeling roller, (°); α and β are the scraping angle of peeling rollers, respectively, (°); γ is the relative angle of peeling rollers, (°); G_1 is the component force along the inclining direction of the peeling roller, N; G_2 is the component force perpendicular to the inclining direction of the peeling roller G, N; f is the friction force of peeling rollers, N; ω_1 is the angular velocity of peeling roller, rad/s. Thus, the frictional force of peeling rollers on ear can be expressed as following respectively.

$$\begin{cases} T_1 = f_1 Q_1 = f_1 \dfrac{G\cos\delta\cos(\alpha-\gamma)}{\sin(\beta+\alpha)} \\ T_2 = f_2 Q_2 = f_2 \dfrac{G\cos\delta\cos(\alpha+\gamma)}{\sin(\beta+\alpha)} \end{cases} \tag{5}$$

where, f_1 and f_2 are the frictional coefficient of up and down peeling rollers on ear. According to the position relationship in Figure 5, the Equation (5) can be arranged as

$$\begin{cases} T_1 = f_1 G\cos\delta \dfrac{\sqrt{4R^2-H^2}-2H\sqrt{(r+R)^2-R^2}}{\sqrt{(r+R)^2-R^2}-\sqrt{(r+R)^2-R^2}(r+R)} \\ T_2 = f_2 G\cos\delta \dfrac{\sqrt{4R^2-H^2}-2H\sqrt{(r+R)^2-R^2}}{\sqrt{(r+R)^2-R^2}-\sqrt{(r+R)^2-R^2}(r+R)} \end{cases} \tag{6}$$

where, H is the height difference between two peeling rollers, mm; r is the mean radius of ear, mm; R is the radius of peeling rollers, mm. Combing the structural characteristics and test results of the above-mentioned peeling device with fixed parameters, the inclination angle of peeling roller δ is determined to be 15°-30°, the relative angle of peeling rollers γ is 19°, the height difference H is 7.3 mm, and the radius of peeling rollers is 37 mm.

In order to improve peeling rate and reduce ear grain loss, two pairs of peeling rollers form a groove arrangement, the structural layout as shown in Figure 6. The clearance between peeling rollers is adjusted by tighten right and left tighten adjusting bolts. The active peeling roller adopts cast iron roller with double spiral structure to transport the ear backward smoothly. The driven peeling roller adopts rubber roller with fish-scale to improve peeling capacity.

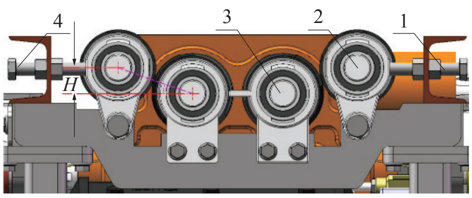

a. Front view

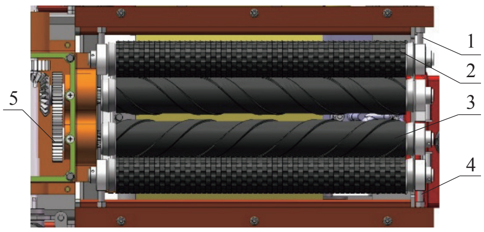

b. Top view

1. Right tighten adjusting bolts 2. Driven peeling roller 3. Avtive peeling roller 4. Left tighten adjusting bolts 5. Transmission gear

Figure 6 Structure diagram of peeling device

2.4 Design of pressure feeding device

The effect of pressure feeding device is to increase the friction between ears and the peeling rollers, and help ears slide to improve the productivity and snapping rate of the peeling device. The pressure feeding device mainly comprises drive chain and three grade pressure feeding rollers, which is shown in Figure 7.

2.5 Design of attitude adjustment device

In order to adapt to the hilly and mountains terrain with large slope, the small maize harvester must have the function of attitude adjustment, leveling the body to improve its safety, ear snapping reliability and operation efficiency. During operation, the lateral force of small maize harvester can cause the body to roll over. The static mechanical model is established assuming that the harvester is rigid body, as shown in Figure 8.

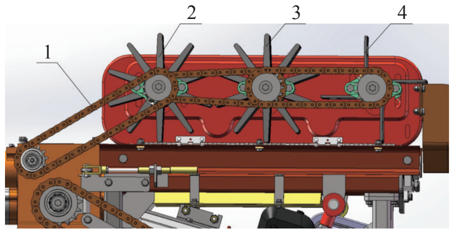

a. Front view

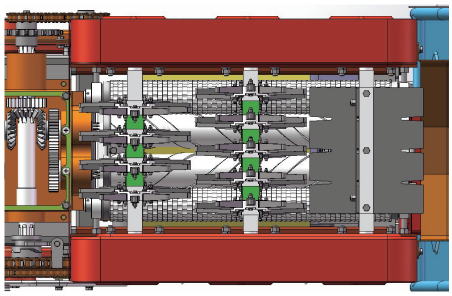
b. Top view

1. Drive chain 2. Ⅰ grade pressure feeding roller 3. Ⅱ grade pressure feeding roller 4. Ⅲ grade pressure feeding roller

Figure 7 Structure diagram of pressure feeding device

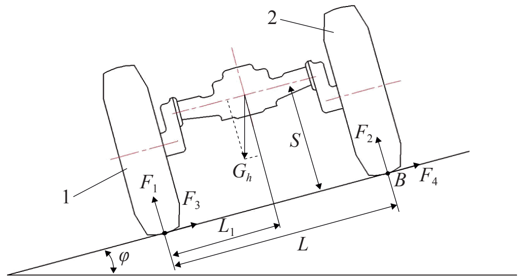

1. Low tire 2. High tire

Figure 8 Static mechanical model of small maize harvester

According to the geometric relationship, the force at the contact point A between the low tire and the ground satisfies is

$$\begin{cases} F_3 + F_4 - G_h\sin\varphi = 0 \\ F_1 + F_2 - G_h\cos\varphi = 0 \\ G_h(L_1 - S\tan\varphi)\cos\varphi - F_2 L = 0 \end{cases} \tag{7}$$

where, G_h is the gravity of the small maize harvester during operation, N; S is the vertical height between the center of gravity of the small maize harvester and the ground, mm; L_1 is the distance from A to the gravity center on slope, mm; L is the wheel base on the slope, mm; φ is the horizontal inclination angle of the ground, (°); F_1 is the ground support force on the low tire, N; F_2 is the ground support force on the high tire, N; F_3 is the frictional force of low tire, N; F_4 is the frictional force of high tire, N.

When the harvester works on the slope with inclination angle of φ, the ground support force on the low and high tire is different. When the harvester rolls over, the high tire gets off the ground firstly. The sign of the harvester turning over is that the ground on the high tire satisfies

$$F_2 = 0 \tag{8}$$

Sorting out Equations (7)-(8) can get:

$$L_1 - S\tan\varphi = 0 \tag{9}$$

Derivation of Equation (9) can get:

$$\varphi_{\max} = \arctan\frac{L_1}{S} \tag{10}$$

where, $\varphi_{\max}$ is the critical stable roll angle of harvester, (°). It can be obtained by Equation (10) that the rollover of small maize harvester working on sloping land is related to the gravity center and the wheel base. However, according to maize planting agronomy, the wheel base L and gravity center height S cannot be optimized.

Therefore, the attitude of the body can be adjusted by raising the rack height on low tire, which is equivalent to leveling the body. The attitude adjustment principle is shown as Figure 9. Based on the above research and analysis, the highest point stationary pursuit leveling method is adopted. By measuring the positive and negative attitude angle of the frame, the position of the high position tire is judged and the high position hydraulic cylinder is kept unchanged. At the same time, the low tire cylinder is controlled to extend and drive the low side frame to rise up, and when the attitude angle of the frame approaches zero, the low cylinder stops its action, and the small maize harvester finally reaches the level state.

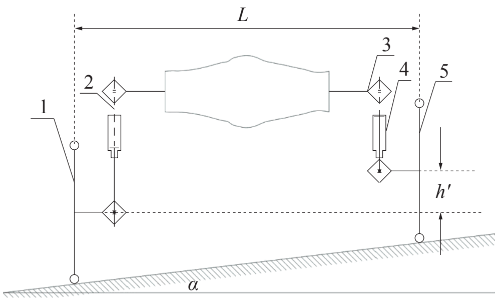

1. Low tire 2. Left swing mechanism 3. Traveling gearbox 4. Hydraulic cylinder 5. High tire

Figure 9 Attitude adjustment principle

For this purpose, the attitude adjustment device mainly consists of hydraulic oil tank, hydraulic oil pump, sewing mechanism and hydraulic cylinder, which is symmetrically arranged on both sides of the body. The side structure is shown in Figure 10.

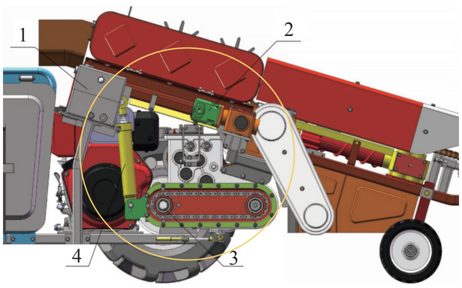

1. Hydraulic oil tank 2. Hydraulic oil pump 3. Right swing mechanism 4. Hydraulic cylinder

Figure 10 Structure diagram of attitude adjustment device

The sewing mechanism adopts a chain drive structure, which can rotate independently. During operation, by extending the length of the low tire hydraulic cylinder, the frame is raised to level, which is the highest point stationary pursuit leveling method. While the angle swing mechanism is controlled to achieve the purpose of stepless adjustment of the tire height difference. At this point, the attitude angle of the frame is 0.

2.6 Design of transmission system

In order to achieve the purpose of compact structure, simplified transmission and lightweight of the small maize harvester, the gearbox of maize snapping and peeling device is integrated. The transmission system arrangement is shown in Figure 11.

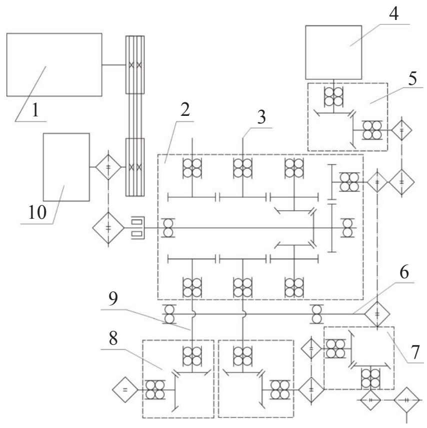

1. Engine 2. Integrated gearbox of snapping and peeling 3. Peeling rollers 4. Vane pump 5. Vane pump reducer 6. Straw crushing shaft 7. Pressing reducer 8. Feeding reducer 9. Straw pulling rollers 10. Traveling reducer.

Figure 11 Transmission system diagram of small maize harvester

The power is divided into two ways by the engine, one way to the walking transmission, the other way to the integrated gearbox of snapping and peeling. As shown in Figure 11, the gearbox sends out three set of power. One way is transmitted to straw crushing device through chain drive, the other to straw pulling rollers through bevel gear drive, and the third to peeling rollers. The straw pulling rollers rotate opposite to each other through the engagement of spur gears. At the same time, the driven straw pulling roller is connected with the pin shaft and the bevel gear mechanism to realize the operation of feeding plant. Finally, the driven chain is used to transfer the power to the peeling and pressure feeding device. The total power is provided by the HP195F diesel engine, which can meet the requirements of production and use.

3 Materials and methods

3.1 Attitude adjustment test

The planting areas in China hilly and mountainous are characterized by slops, but low-lying bumps are not obvious, and the harvester has the risk of rollover, so it is necessary to focus on the leveling of the left and right sides of the body.

The device to verify the leveling effect consists of an attitude detection system and a laptop. The attitude detection system consists of the MPU 6000 sensor to detect the attitude change of the frame and 170 telescopic displacement sensor to detect the displacement of the two sides cylinders. MPU 6000 sensor is arranged in the center of the frame to represent the attitude of the small maize harvester. The plane of the MPU 6000 must be parallel to the installation platform, the *x*-axis was in line with the forward direction, and the *y*-axis is perpendicular to *x*-axis. During harvesting, the left side of the person is defined as the left side of the small harvester. When the left tire is the high tire, the attitude angle λ is negative and conversely, λ is positive, as shown in Figure 12. In particular, when the body is horizontal, λ is 0°.

In order to test actual range of attitude adjustment and the accuracy of static attitude adjustment, the following tests were designed.

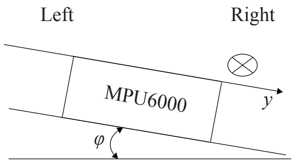

Figure 12 Attitude of small maize harvester

Firstly, two groups of tests were carried out to push the left and right hydraulic cylinders to the limit position respectively to test the actual adjustment range. When the cylinder reached the limit position, the attitude detection system was used to detect the body attitude. The upper computer can directly display the rotation angle around x and y axis measured by the sensor.

Secondly, another two groups of tests were carried out with the small harvester placed forward and backward in the test field. The slop angle ψ of the test field was about 13.8°, which was in a professional planting cooperative in Juxian, Shandong Province. That is to say, the attitude angles of the body were +13.8° and –13.8° during tests, respectively. Flatten the body separately and test the attitude adjusting precision and speed of the body.

3.2 Field harvesting test

To test the harvesting performance of the small maize harvester with attitude adjustment in China hilly and mountain areas, the field harvesting test were conducted in the experimental field during July, 2021. Test equipment included the small maize harvester, 30 m tape measure, TL-4 intelligent moisture tester, J9-2 stopwatch, HCS-50 electronic crane scale, JJ3000 electronic balance, TEST0410-2 digital anemometer, steel ruler, vernier caliper, and other tools. The length of test field was 60 m and the spacing 60 cm. The main planting variety waxy maize Tiangui 932 was selected as the test material. The physical characteristics of its harvest period was that the average moisture content of grain 33.6%, the average moisture content of straw 87%, the average moisture content of maize ear 50%, the plant lodging rate below 2.3%, the ear droop rate below 5%, the minimum heading height above 360mm. Before the field harvesting test, the body should be adjusted firstly. The test process was shown in Figure 13.

Figure 13 Field experiment process

In the operation, the operation effect was mainly determined by the maize damage rate and loss rate. The results showed that the rotational speed of straw pulling rollers, peeling rollers and pressure feeing rollers were the main factors affecting the effect of maize harvesting. The maize snapping device has an important effect on snapping performance of the small harvester. In order to reduce the snapping loss and ear damage, it is necessary to determine the appropriate rotational speed of straw pulling rollers. According to the theoretical analysis of maize snapping process, the rotational speeds of straw pulling rollers are selected as 1200, 1500 and 1800 r/min. In order to improve the peeling performance and efficiency of the peeling device, the rotational speed of peeling rollers should not be small. According to the practical experience, the rotational speeds of peeling rollers are selected as 1200, 1500 and 1800 r/min respectively. The pressure feeding device also has a significant effect on the peeling effect of ears, and the appropriate rotational speed of the pressure feeding rollers can improve the bract peeling rate. Based on the harvesting performance of the small harvester in the actual production operation, the rotational speed of pressure feeding rollers are selected as 300, 400 and 500 r/min for test.

The test was based on the Box-Behnken orthogonal table[23], with the rotational speed of straw pulling rollers, peeling rollers and pressure feeding rollers as the experimental factors, and ear loss rate and bract peeling rate as evaluation indicators[24,25]. The coding table of experimental factors is listed in Table 2.

Table 2 Actual value and code of the variable

Levels	Rotational speed of straw pulling rollers x_1/r·min^{-1}	Rotational speed of peeling rollers x_2/r·min^{-1}	Rotational speed of peeling rollers x_3/r·min^{-1}
–1	1200	1200	300
0	1500	1500	400
1	1800	1800	500

The forward distance of the small maize harvester is 20 m and each test was repeated 3 times. Following the regulations of the Chinese National Standard[26,27], the evaluation indicators used for the assessment of maize harvested in the test are defined:

1) Measurement of the ear loss rate

The rate of ear loss is a measure of ears missing and falling the process of harvesting. The ear loss rate is calculated as Equation (11):

$$Y_1 = \frac{m_1}{m_e} \times 100\% \tag{11}$$

where, Y_1 is the ear loss rate, %; m_1 is the mass of the missing and falling ears measured in the test, kg; m_e is the total mass of the ears measured in the test, kg.

2) Measurement of the bract peeling rate

The rate of bract peeling is a measure of ear in the harvesting, ear of bracts with more than three (more than two-thirds of the whole leaf counts as one). The bract peeling rate is calculated as Equation (12):

$$Y_2 = \frac{m_e - m_2}{m_e} \times 100\% \tag{12}$$

where, Y_2 is the bract peeling rate, %; m_2 is the mass of unstripped ears measured in the test, kg.

4 Results and discussion

4.1 Attitude adjustment test results and analysis

The actual adjustment range of attitude angle is listed in Table 3. The adjustment range of the attitude angle is from –16.34° to 16.12°, which can meet the demand of the attitude adjustment of most hills and mountains. When the small harvester is on a level road, the output data of the sensor is regarded as the error caused by uneven installation, which is used to correct and compensate attitude adjustment errors. The test results for the static attitude adjustment are shown Figure 14.

Table 3 Actual attitude adjustment range

State	x-axis attitude angle/(°)	y-axis attitude angle/(°)
Level road	–0.24	–0.06
Leaning to the right	1.135	–16.34
Leaning to the left	1.335	16.12

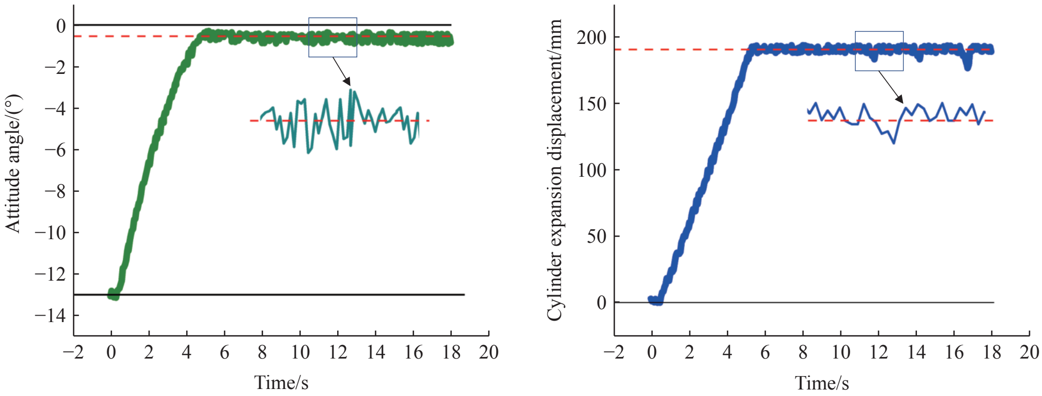

a. Leaning to the right

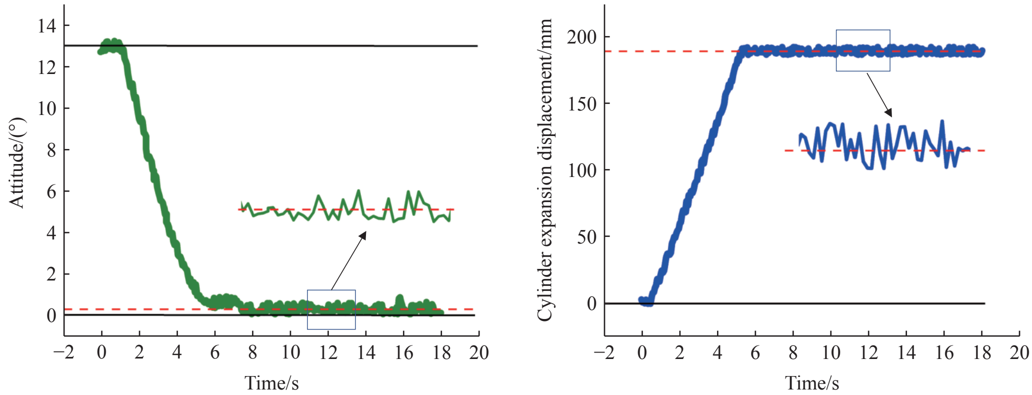

b. Leaning to the left

Figure 14 Attitude angle and cylinder adjustment process of right and left tilting

As depicted in Figure 14a, the attitude angel of the small harvester leaning to the right before and after the attitude adjustment is –13.582° and –0.265°. The expansion displacement of the right cylinder is 187.532 mm and the response time of the adjusting process is approximately 4.855 s. Because of the high sensitivity of the sensor, the data fluctuates in a small range when the attitude angel tends to be stable.

As depicted in Figure 14b, the attitude angel of the small harvester leaning to the left before and after the attitude adjustment is 13.625° and 0.289°. The expansion displacement of the left cylinder is 188.019 mm and the response time of the adjusting process is approximately 5.234 s. It can be seen that the accuracy of attitude adjustment is higher when the harvester leaning to the left. The reason may be that the weight on the left side of the small harvester is slightly smaller.

The attitude adjustment performance tests show that the attitude adjustment range is smaller than the target range due to the assembly error of the attitude adjustment device and the excessively high body tilting. Actually, when the field slope exists, the field incline would increase degree of the body, resulting in the frame unable to achieve leveling. However, the farmland in hilly and mountain areas is generally built on horizontal terraced fields, the body tilt will not exceed the limit to adjust the angle, which can basically achieve the purpose of leveling.

4.2 Field harvesting test results and analysis

4.2.1 Test results

The Design-Expert 10.0.1 software was used to Design the test scheme and analyze the results. In order to reduce the test error, each group of tests was repeated 3 times, and the average value was taken as the test result. Table 4 lists the test scheme and results.

4.2.2 Establishment of regression model and significance analysis

In order to explore the optimal operating parameters of the small maize harvester after attitude adjusted, based on the test data in Table 4, Design-Expert 10.0.1 software was used to perform a multivariate regression fitting analysis and establish a response surface regression model with three independent variables. The analysis of variance is listed in Table 5.

Table 4 Test scheme and results

No.	Rotational speed of straw pulling rollers X_1	Rotational speed of peeling rollers X_2	Rotational speed of pressure feeding rollers X_3	Ear loss rate Y_1/%	Bract peeling rate Y_2/%
1	–1	–1	0	2.01	92.80
2	1	–1	0	3.89	93.20
3	–1	1	0	3.12	95.30
4	1	1	0	4.52	96.10
5	–1	0	–1	2.42	92.20
6	1	0	–1	4.12	93.90
7	–1	0	1	3.20	94.60
8	1	0	1	4.32	95.10
9	0	–1	–1	3.23	92.70
10	0	1	–1	2.98	96.30
11	0	–1	1	2.57	94.80
12	0	1	1	3.60	96.60
13	0	0	0	1.18	93.90
14	0	0	0	1.59	93.80
15	0	0	0	1.23	93.70
16	0	0	0	1.48	94.10
17	0	0	0	1.36	93.80

Note: X_1, X_2, and X_3 are the level values of experimental factors.

It can be found from Table 5 that the model of ear loss rate Y_1 and bract peeling rate Y_2 were less than 0.001, proving that the regression equation was significant and the experimental design was reliable. The lack of fit of ear loss rate Y_1 and bract peeling rate Y_2 were 0.1505 and 0.0925, respectively, which were greater than 0.05, proving that the regression equations fit very well. Therefore, the results obtained using the regression equations could be used to replace the actual results of the test. With the insignificant factors eliminated, the second-order multiple regression equations for the coding factors were obtained.

Table 5 Variance analysis of target rate

Items	Sources	Sum of squares	Degree of freedom	Mean squares	F-values	p-values
Y_1	Model	20.09	9	2.23	40.27	<0.0001**
	x_1	4.65	1	4.65	83.92	<0.0001**
	x_2	0.79	1	0.79	14.32	0.0069*
	x_3	0.11	1	0.11	1.99	0.2009
	x_1x_2	0.058	1	0.058	1.04	0.3419
	x_2x_3	0.084	1	0.084	1.52	0.2578
	x_1x_3	0.41	1	0.41	7.39	0.0298*
	x_1^2	6.25	1	6.25	112.79	<0.0001**
	x_2^2	2.68	1	2.68	48.44	0.0002**
	x_3^2	3.63	1	3.63	65.49	<0.0001**
	Residuals	0.39	7	0.055		
	Lack of fit	0.27	5	0.091	3.12	0.1505
	Errors	0.12	4	0.029		
	Total	20.47	16			
Y_2	Model	25.76	9	2.86	50.47	<0.0001**
	x_1	1.44	1	1.44	25.48	0.0015
	x_2	14.58	1	14.58	257.08	<0.0001**
	x_3	4.5	1	4.5	79.35	<0.0001**
	x_1x_2	0.04	1	0.04	0.71	0.4288
	x_2x_3	0.36	1	0.36	6.35	0.0398
	x_1x_3	0.81	1	0.81	14.28	0.0069
	x_1^2	0.46	1	0.46	8.08	0.0249
	x_2^2	2.83	1	2.83	49.92	0.0002
	x_3^2	0.74	1	0.74	13.10	0.0085
	Residuals	0.4	7	0.057		
	Lack of fit	0.31	3	0.1	4.42	0.0925
	Errors	0.092	4	0.023		
	Total	26.16	16			

Note: $p<0.01$ (highly significant, **); $p<0.05$(significant, *)

The regression equation of ear loss rate Y_1 is

$$Y_2 = 93.86 + 0.42x_1 + 1.35x_2 + 0.75x_3 - 0.3x_1x_3 - 0.45x_2x_3 - 0.33x_1^2 + 0.82x_2^2 + 0.42x_3^2 \quad (13)$$

The regression equation of bract peeling rate Y_2 is

$$Y_2 = 93.86 + 0.42x_1 + 1.35x_2 + 0.75x_3 - 0.3x_1x_3 - 0.45x_2x_3 - 0.33x_1^2 + 0.82x_2^2 + 0.42x_3^2 \quad (14)$$

4.2.3 Analysis of interaction results

It can be seen from Table 5 that the significant effects of rotational speed of straw pulling rollers, peeling rollers and pressure feeding rollers on ear loss rate Y_1 are in a decreasing order. When the rotational speed of straw pulling is too high, the collision between maize ears and snapping plats would occur in the process of snapping, resulting in the damage of maize ears directly. The significant effects of the rotational speed of peeling rollers, pressure feeding rollers and straw pulling rollers on bract peeling rate Y_2 are in a decreasing order. The effect of rotational speed of straw pulling on bract peeling rate is relatively small, because the peeling process is after the snapping process.

The interaction term X_2X_3 of rotational speed of peeling rollers X_2 and rotational speed of pressure feeding rollers X_3 have a significant effect both on the ear loss rate Y_1 and bract peeling rate Y_2, indicating that there are interaction effects among all factors. Figure 15 shows the response surface of the interactive factors that affect the test indicators.

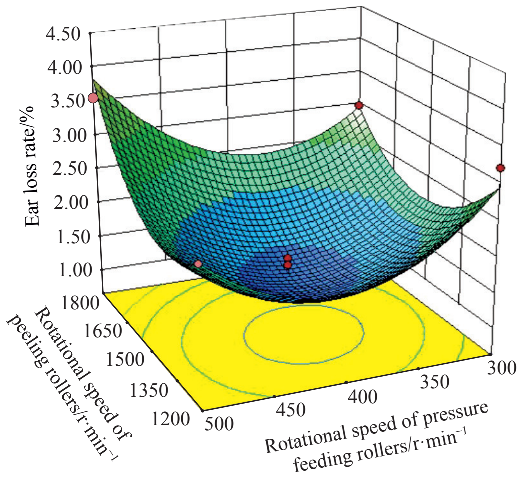

a. $Y_1=f(1500, X_2, X_3)$

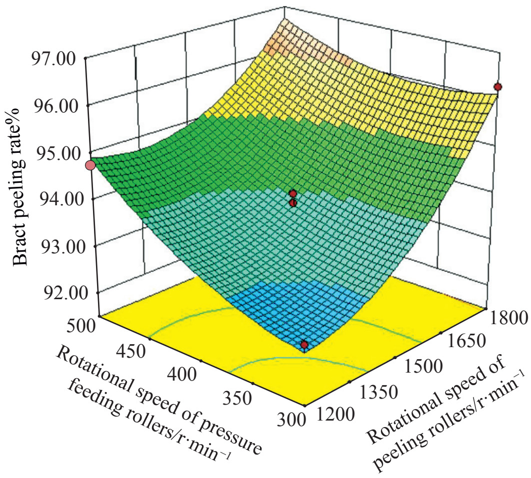

b. $Y_2=f(1500, X_2, X_3)$

Figure 15 Effect of interaction factors on ear loss rate and bract peeling rate

In Figure 15a, at the same rotational speed of pressure feeding rollers, the ear loss rate decreases first and then increases rapidly with the rotational speed of peeling rollers. When the rotational speed of peeling rollers was high, the ears were easy to jump on the peeling rollers and then the peeling rollers caused damage on the ears directly during the peeling process. At the same rotational speed of peeling rollers, the ear loss rate decreases first and then increases slightly with the rotational speed of pressure feeding rollers. When the rotational speed of pressure feeding rollers was high, the contact time between the peeling rollers and ears increased, which increased the ear loss rate and easily caused plug.

In Figure 15b, at the same rotational speed of pressure feeding rollers, the bract peeling rate increased gradually with the rotational speed of peeling rollers. When the rotational speed of peeling rollers was too small, the peeling rollers were difficult to peel off the bracts, and the productivity was low, it was difficult to meet the production demand. At the same rotational speed of peeling rollers, the bract peeling rate increases rapidly at low rotational speed of peeling rollers and increases slowly at high rotational speed of peeling rollers with the rotational speed of pressure feeding rollers. With the increase of the rotational speed of pressure feeding rollers, the ears on the peeling rollers tended to fluctuate up and down, which leaded to the decrease of the contact time between the peeling rollers and maize, and the corresponding reduction of the bract peeling rate.

4.2.4 Parameter optimization and test verification

In order to explore the optimal relationship between the test indicators and the main influencing factors, the multi-objective optimization method was adopted to analyze the optimal parameter combinations. According to the target of improving the bract peeling rate and reducing the ear loss rate, combined with the boundary conditions of each experimental factors, the optimization model was obtained as follows:

$$\begin{cases} \min Y_1 \\ \max Y_2 \\ \text{s.t.} \begin{cases} x_1 \in (1200, 1800) \\ x_2 \in (1200, 1800) \\ x_3 \in (300, 500) \end{cases} \end{cases} \tag{15}$$

Through the solution of the Design-Expert software 10.0.1, the best combination was obtained: the rotational speed of straw pulling rollers, peeling rollers and pressure feeding rollers are 1434.13 r/min, 1534.02 r/min and 405.91 r/min. At this time, the ear loss rate and bract peeling rate are 1.32% and 93.95%.

To verify the accuracy of the optimized model, the parameters of the optimized factors were tested in the field. Considering the practical application of the small maize harvester, the above parameters were rounded as follows: the rotational speed of straw pulling rollers, peeling rollers and pressure feeding rollers were 1440 r/min, 1535 r/min and 406 r/min. After substituting into the regression equations, the predicted ear loss rate and bract peeling rate were 1.33% and 93.98%.

In order to verify the optimization analysis results, a validation test was carried out on the ear loss rate and bract peeling rate under the optimal combination of factors. The test was repeated for 10 times to eliminated random error and the test results were averaged. The measured results showed that the ear loss rate and bract peeling rate were 1.39% and 94.22%. Comparing the measured and predicted values, the relative errors of all property indices were less than 5%, which showed that the model was reliable and can be used for prediction and optimization.

5 Conclusions

1) In this study, a small maize harvester with attitude adjustment was designed for mechanized maize harvesting in China hilly and mountainous areas. The basic structure and working principle of the small maize harvester were described, and the key components of maize snapping device, peeling device, pressure feeding device, transmission system and attitude adjustment advice were designed.

2) The attitude adjustment advice was designed according to the high point stationary pursuit leveling method. The actual range of attitude adjustment was obtained and the accuracy of static attitude adjustment was verified through attitude adjustment test. The attitude adjustment performance tests show that the attitude adjustment range is smaller than the target range due to the assembly error of the attitude adjustment device and the excessively high body tilting.

3) A prototype of the small maize harvester with attitude adjustment was assembled and test in the field. Field experiment results showed that when the rotational speed of straw pulling rollers, peeling rollers and pressure feeding rollers were 1440 r/min, 1535 r/min and 406 r/min, the ear loss rate and bract peeling rate were 1.33% and 93.98%, which satisfying the need of maize mechanized harvesting in China hilly and mountainous areas.

Moreover, the small maize harvester with attitude adjustment has strong practicability. Furthermore, the research on the attitude adjustment of the small maize harvester is elevated to a certain extent. In order to validate the reliability of the attitude adjustment of the small harvester, more experimental tests need to be carried out in areas with large lateral slope variations.

Acknowledgements

This work was financially supported by the Shandong Provincial Natural Science Foundation (Grant No. ZR2023QE091), and the Shandong Province Agricultural Machinery R&D Manufacturing Promotion and Application Integration Project (Grant No. NJYTHSD-202318).

[References]

[1] Liu G S, Zhao L S, Cheng Y X, Zhou Y T, Wang C Y, Lin H B, et al. Land consolidation zoning of Northern Guangdong for suitable mechanization transformation in hilly and mountainous areas based on limiting factors. Transactions of the CSAE, 2021; 37(12): 262–270. (in Chinese)

[2] Yang F, Du Y F, Fu Q F, Li X Y, Li Z, Mao E R, et al. Design and testing of seed maize ear peeling roller based on Hertz theory. Biosystems Engineering, 2021; 202: 165–178.

[3] Geng D Y, Sun Y C, Li H B, Mou X D, Zhang G D, Wang Z Y, et al. Design and experiment of crawler corn harvester for sloping field. Transactions of the CSAE, 2021; 37(13): 11–19. (in Chinese)

[4] Cheng X P, Jia X D, Chen M Z, Li Q Y. Experiment and analysis on test device of corn ear picking by pulling stalk upward. Transactions of the CSAE, 2016; 32(22): 50–55. (in Chinese)

[5] Qin J H, Yin Y P, Liu Z G, Du Y F, Wang G Y, Zhu Z X, et al. Optimisation of maize picking mechanism by simulation analysis and high-speed video experiments. Biosystems Engineering, 2020; 189: 84–98.

[6] Du Y F, Fu S H, Mao E R, Zhu Z X, Li Z. Development situation and prospects of intelligent design for agricultural machinery. Journal of Agricultural Mechanization Research, 2019; 50(9): 1–20. (in Chinese)

[7] Sun Z Z, Yang Y F, Qi Y Y, Wang P P. Design and test of small corn harvester. Journal of Agricultural Mechanization Research, 2018; 40(11): 176–179, 184. (in Chinese)

[8] Tang Z F, Liu S P, Zhou F J, Li T Y, Wang J L, Li C Y. Design and experiment of ear harvester for seed corn. Transactions of the CSAM, 2021; 52(7): 102–112. (in Chinese)

[9] Tulpule P, Kelkar A. Integrated robust optimal design (IROD) of header height control system for combine harvester. 2014 American Control Conference. Portland: IEEE, 2014; 26699-2704.

[10] Geng D Y, He K, Wang Q, Jin C Q, Zhang G H, Lu X F. Design and experiment on transverse axial flow flexible threshing device for corn. Transactions of the CSAM, 2019; 50(3): 101–108. (in Chinese)

[11] Li T Y, Guan X D, Zhou F J. Mechanistic analysis and experimental study of a shear-type low-loss fresh corn ear-picking mechanism. Computers and Electronics in Agriculture, 2023; 213: 108191.

[12] Quick G R. Single-pass corn and stover harvesters: development and performance. Proceeding of International Conference on Corp Harvesting and Processing, Louisville, Kentucky, USA, 2003.

[13] Willcutt H. Corn harvesting, drying, and storage: extension service of Mississippi. Cooperating with U. S. Department of Agriculture, 2001; 41(5): 37–41.

[14] Yao Y C, Liu Y Y, Niu G D, Zhang Y P, Geng D Y, Diao P S. Economic benefit analysis and evaluation method of wheat maize whole mechanization technology mode in dry farming irrigation area of Shandong Province. Journal of Chinese Agricultural Mechanization, 2020; 41(12):

6–11. (in Chinese)

[15] Zhao R Q, Fu J, Chen Z, Tian L, Ren L Q. Low-rank-constraint-based machine vision algorithm for chaffer-sieve-clogging recognition of corn harvester. Computers and Electronics in Agriculture, 2022; 198: 107056.

[16] Zhang L H, Luo H Z, Zhou Y, Qiu Q Y, Yuan S L, Cai J X. Design and test of bionic crushing blade based on the mandible of the leaf-cutter ant for harvesting silage maize. Transactions of the CSAE, 2022; 38(12): 48–56. (in Chinese)

[17] Xu H G, Zhang C X, Zhang X J, Wang J Q. Development and application of corn harvester for hilly area. Agricultural Engineering, 2021; 11(3): 102–107. (in Chinese)

[18] Messenbet G, Aynadis M, Nigus G, Jaggar H, Rizana M, Fetien A. Effects of threshing and storage conditions on post-harvest insect infestation and physical characteristics of maize grain. Journal of Stored Products Research, 2023; 103: 102131.

[19] Yang Z F, Niu H L, Sun J B, Liu Z J, Li Y L, Chu H L. Design and experiment of attitude cooperative control system of mountain Crawler tractor and farm tools. Transactions of the CSAM, 2022; 53(1): 414–422. (in Chinese)

[20] Liu Z, Zhang G, Chu G, Niu H, Zhang Y, Yang F et al. Design matching and dynamic performance test for an HST-based drive system of a hillside crawler tractor. Agriculture, 2021; 11(5): 466.

[21] Li T Y. Design and experiment on flexible low-loss fresh corn picking device. Master dissertation. Harbin: Northeast Agricultural University, 2019; 72p. (in Chinese)

[22] Xie R Z, Ming B, Gao S, Wang K R, Hou P, Li S K. Current state and suggestions for mechanical harvesting of corn in China. Journal of Integrative Agriculture, 2022; 21(3); 892–897.

[23] Ge Y Y, Liang Q Y, Wang G L. Experimental design method and application of Design-Expert software. Harbin: Harbin Institute of Technology Press, 2015; 214p. (in Chinese)

[24] GB/T 21962-2020. Corn combine harvester. National Standards of the People's Republic of China. 2021; 48p. (in Chinese)

[25] GBT 34379-2017. Technical specifications for mechanized production of corn. National Standards of the People's Republic of China. 2017; 6p. (in Chinese)

[26] Zhao J L, Zhao H N, Tang H, Wang X P, Yu J J. Bionic threshing component optimized based on MBD-DEM coupling simulation significantly improves corn kernel harvesting rate. Computers and Electronics in Agriculture, 2023; 212: 108075.

[27] Jin C Q, Yang T X, Liu G H, Wang T E, Chen M, Liu Z. Design and test of posture controlled chassis for caterpillar combine. Transactions of the CSAM, 2020; 51(11): 393–402. (in Chinese)